nature geoscience

LETTERS

PUBLISHED ONLINE: 1 APRIL 2012 | DOI: 10.1038/NGEO1427

Terrestrial carbon isotope excursions and biotic change during Palaeogene hyperthermals

Hemmo A. Abels[1]*, William C. Clyde[2], Philip D. Gingerich[3], Frederik J. Hilgen[1], Henry C. Fricke[4], Gabriel J. Bowen[5] and Lucas J. Lourens[1]

Pronounced transient global warming events between 60 and 50 million years ago have been linked to rapid injection of isotopically-light carbon to the ocean–atmosphere system[1,2]. It is, however, unclear whether the largest of the hyperthermals, the Palaeocene–Eocene Thermal Maximum (PETM; ref. 3), had a similar origin[4,5] as the subsequent greenhouse climate events[1,6], such as the Eocene Thermal Maximum 2 and H2 events. The timing and evolution of these events is well documented in marine records[7,8], but is not well constrained on land. Here we report carbon isotope records from palaeosol carbonate nodules from the Bighorn Basin, Wyoming, USA that record the hyperthermals. Our age model is derived from sedimentary cyclostratigraphy, and shows a similar structure of events in the terrestrial and marine records. Moreover, the magnitude of the terrestrial isotope excursions is consistently scaled with the marine records, suggesting that the severity of local palaeoenvironmetal change during each event was proportional to the size of the global carbon isotope excursion. We interpret this consistency as an indication of similar mechanisms of carbon release during all three hyperthermals. However, unlike during the PETM (refs 9,10), terrestrial environmental change during the subsequent hyperthermals is not linked to substantial turnover of mammalian fauna in the Bighorn Basin.

Palaeoclimate research recognizes the importance of past rapid and transient global warming events, so-called hyperthermals, as potential analogues for present-day climate change[2,11,12]. The Palaeocene–Eocene Thermal Maximum (PETM) at ~56 million years ago represents the most prominent of these events and is characterized by a rapid global temperature rise of 5–9 °C in ten thousand years that gradually declined to pre-excursion values in ~100–200 thousand years[12]. The temperature rise during the PETM is associated with a carbon isotope excursion (CIE) of 2–6.5‰, pointing to the release of >2,000 Gigatons of carbon[6,11–13]. This disruption of Earth's carbon cycle and climate system had wide-ranging effects on continental hydrology, the chemistry of the ocean, and global biotas[3,9,10,14,15]. Deep marine records reveal the existence of other, smaller amplitude anomalies that mimic the PETM (refs 1,4,6). Eocene Thermal Maximum 2 (ETM2) is also known as H1 and is associated with the Elmo clay layer in the deep marine realm[1]. The event is associated with the second largest CIE identified in the early Palaeogene marine record thus far[1], and corresponds to even greater high-latitude temperatures than the PETM (ref. 16). ETM2 is followed by the smaller H2 event, around 100 thousand years later[1,6,7,17].

We report the detailed evidence for ETM2 and H2 in continental successions located in the McCullough Peaks area of the Bighorn Basin, Wyoming, U.S.A. The well-known fossil-rich sedimentary archives of this basin have previously revealed important details on the terrestrial climatic and biotic impact of the PETM (refs 3,9,15, 18,19). Early Eocene sediments of the Willwood Formation were deposited on the floodplains of meandering river systems. Fine-grained overbank deposits show striking colour banding related to ancient soil horizons with different maturity, styles and spacing[18,19]. The Upper Deer Creek (UDC and Supplementary Figs S3a and S4) and Gilmore Hill (GH and Supplementary Fig. S5) sections studied here are ~17 km apart (Supplementary Figs S1 and S2) and were selected for their excellent outcrops, lack of sandstone bodies at UDC, and rich mammalian fossil localities in or near the section at GH (Fig. 1 and Supplementary Table S3). Palaeosol carbonate nodules were sampled every ~10–70 cm and carbon isotope ratios were measured ($\delta^{13}C_{pc}$ and Supplementary Tables S1 and S2).

The UDC section is characterized by two negative $\delta^{13}C_{pc}$ excursions of −3.8‰ and −2.9‰ whereas the GH section is characterized by one negative $\delta^{13}C_{pc}$ excursion of −2.7‰ (Fig. 1). Previous work on late Palaeocene—early Eocene palaeosols of the Willwood Formation[20] has shown that pedogenic carbonates in these soils formed below the zone of strong diffusive mixing between atmospheric and soil CO_2, meaning that their carbon isotope ratios should track those of palaeovegetation and thus the ocean–atmosphere system[14,20]. The pattern of the negative CIEs at UDC, and their stratigraphic proximity to the Chron C24r-C24n.3n magnetic polarity reversal and to the Wasatchian 4–Wasatchian 5 biozone boundary allows correlation of the larger CIE at UDC to ETM2 and the smaller CIEs at UDC and GH to H2 (refs 8,21; Fig. 1 and Supplementary Figs S6 and S7). The −3.8‰ CIE in the Bighorn Basin for ETM2 is in the range of the −3 to −4‰ CIE found in dispersed organic matter in lignites from a low-resolution terrestrial record of western India[22].

The discovery of terrestrial equivalents of ETM2 and H2 implies that these events, analogous to the PETM, had a major impact on the continental carbon cycle, and observations from the study sections suggest that terrestrial environmental conditions were perturbed during each event as well[1,2,11]. Distinctive thick purple B-horizons of palaeosols that occur within the ETM2–H2 stratigraphic intervals at UDC and GH are primarily constrained to the hyperthermal events. Furthermore, this interval is characterized by increased development of channel sandstone complexes and large mud-filled scours (Supplementary Fig. S5). The regional significance of these lithological changes has not yet been evaluated, but they could relate

[1]Department of Earth Sciences, Utrecht University, 3584 CD, Utrecht, The Netherlands, [2]Department of Earth Sciences, University of New Hampshire, Durham, New Hampshire 03824, USA, [3]Department of Earth and Environmental Sciences, University of Michigan, Ann Arbor, Michigan 48109, USA, [4]Department of Geology, Colorado College, Colorado Springs, Colorado 80903, USA, [5]Department of Earth and Atmospheric Sciences, Purdue University, West Lafayette, Indiana 47907, USA. *e-mail: abels@geo.uu.nl.

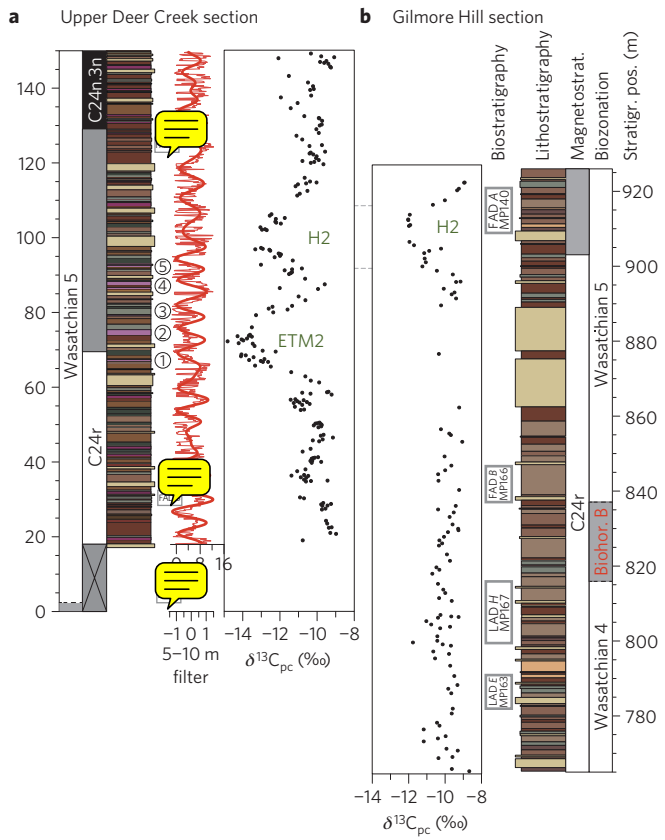

Figure 1 | Terrestrial carbon isotope records of the ETM2 and H2 hyperthermal events. Isotope results are from palaeosol carbonate in the Upper Deer Creek and Gilmore Hill sections in the Bighorn Basin, Wyoming, USA. Stratigraphic thickness is equally scaled for both sections. Magnetochrons and biozonation are given. Five distinct purple beds (1–5) are labelled at UDC (Fig. 2). The bandpass filter of the redness (a*) matrix colour reflectance record is given to denote precession-scale cyclicity. Fossil finds at UDC, and fossil localities (MP) at GH with first and last appearances (FAD and LAD) are given. *A* for *Anacodon*, *B* for *Bunophorus*, *E* for *Ectocion*, and *H* for *Haplomylus*. The correlation between UDC and GH is based on aligning the H2 event. Note that Biohorizon B occurs well before the environmental disturbance related to the hyperthermal events.

to specific environmental conditions on the floodplain, which are not replicated regionally in the time preceding or following the global warming episodes.

Distinct lithologic changes are found in the ETM2–H2 stratigraphic interval in the Bighorn Basin, but biostratigraphic results from this interval do not indicate major faunal changes such as those found through the PETM (refs 3,9,10). Marked turnover in mammalian fossil assemblages has been reported at Biohorizon B across the Wasatchian 4 to Wasatchian 5 biozone boundary[23,24], and some have speculated that this may have been caused by ETM2 (refs 21, 24). Similar to the turnover at the PETM, Biohorizon B exhibits a peak in first and last appearances of mammal taxa that caused an increase in diversity[24]. The extinction of *Haplomylus* and *Ectocion*, two abundant genera that originated before the PETM, and the first appearance of *Bunophorus*, a member of one of the 'modern' order of mammals (Artiodactyla) that first appeared during the PETM, are the primary biostratigraphic criteria originally used to identify Biohorizon B (Supplementary Information; ref. 23). In the GH section, the lowest occurrence of *Bunophorus* is constrained to fall within ~35 m of the highest occurrences of *Haplomylus* and *Ectocion* making it one of the stratigraphically best resolved records of Biohorizon B (Fig. 1 and Supplementary Fig. S2 and Table S3). Although sample sizes of the fossil assemblages collected directly within the GH line of section limit the precision with which Biohorizon B can be positioned in that section (Supplementary Table S3), other fossil assemblages from nearby and *Bunophorus* finds at UDC independently corroborate the GH results (Fig. 1; Supplementary Information). Biohorizon B occurs some 60 m below and ~150–200 kyr before ETM2, showing that the climate change associated with this event did not cause the faunal turnover.

The floodplain succession of the Willwood Formation in the Bighorn Basin is characterized by distinct cyclicity, at a scale of 6–9 m, of alternating (1) fine mudstones, on which mature palaeosol profiles developed; and (2) heterolithic sandy intervals that show only weak pedogenesis. This cyclicity has been related to orbital climate forcing due to the ~21-kyr precession cycle and has already been used to construct an independent internal timescale for the terrestrial PETM (ref. 18). In the UDC section, this scale of lithological rhythmicity is also observed (Fig. 1). Detailed lithological observations complemented with high-resolution records of matrix colour of the sediment reveal 18 (and up to 20) precession cycles in the section with a period of around 7.0 (down to 6.3) metres. Cycle counts indicate the presence of 4–5 precession cycles between ETM2 and H2, supporting marine astronomical age models developed for these hyperthermals[7,25].

For comparison with the marine realm, we constructed a composite $\delta^{13}C$ benthic stack from ODP Sites 1262, 1263, 1265, and 1267 of the Walvis Ridge in the south Atlantic[8] and plotted the data against a previously constructed relative age model[7,8]. Subsequently, we tied the onset of both CIEs from the Bighorn Basin to Walvis Ridge and extrapolated the relative age model of the $\delta^{13}C_{pc}$ record by using the precession-related cycles in lithology and colour reflectance as constraints (Fig. 1). The comparison between the deep marine and continental realms highlights the close similarity between the large-scale carbon isotope changes across both hyperthermals (Fig. 2).

Rapid input of isotopically-depleted carbon into the ocean–atmosphere system was responsible for ocean acidification and the characteristic CIEs (ref. 12) during the hyperthermal events, and undoubtedly contributed to the associated greenhouse warming. The exact amount, isotopic signature, and source(s) of the carbon fuelling the PETM and later hyperthermal events are still unknown[5,11–13]. Also, various carbonate and organic-matter proxies of marine and continental realms record the carbon isotope value of their surrounding carbon pool differently and thus even the true magnitude of the CIE for the mixed ocean–atmosphere carbon pool remains to some degree enigmatic[5,12].

We compare the continental CIEs recorded by Bighorn Basin soil carbonates for PETM, ETM2 and H2 with equivalent records from bulk carbonate and the benthic foraminifer *Nuttallides truempyi* from Walvis Ridge in the southern Atlantic, and bulk carbonate from shallow marine sequences in New Zealand[17,27,28] (Fig. 3 and Supplementary Table S6). Our results show that the amplitudes of each of the three CIEs in the continental soil carbonate records are larger than, and seem to scale linearly with, CIE magnitudes of these marine proxy records.

CIE recording in palaeosol carbonate is dependent on the $\delta^{13}C$ value of the atmosphere, on plant ecophysiology, and on soil properties such as temperature and moisture[12,14], while bulk carbonate and benthic foraminiferal $\delta^{13}C$ records are impacted by ocean circulation and acidification[26,29], among other factors. These effects on CIE magnitude reflect changing local environmental parameters that, during the hyperthermal events, probably occurred in direct or indirect response to carbon input to the ocean–atmosphere system. This addition of isotopically-light carbon is in turn recorded by the CIEs.

The consistent scaling we observe between CIEs in the different proxy records suggests proportionality between the severity of local

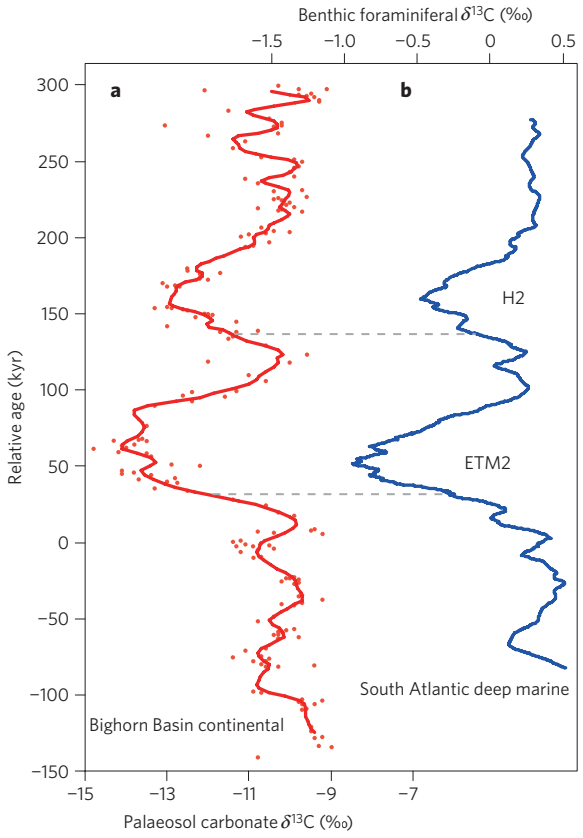

Figure 2 | Carbon isotope records in the continental and marine realms on independent astronomical timescales. a, Continental data are from palaeosol carbonate in the Upper Deer Creek section. Solid line represents a 5-point moving average. **b**, Marine data are from benthic foraminifera and shows a 4-kyr average from a stacked record of Ocean Drilling Program Sites 1262, 1263, 1265, 1267 (Walvis Ridge, southern Atlantic Ocean). Note the great similarity between the deep marine and the continental carbon isotope records indicating both coincidently recorded the carbon isotope signature of the global ocean–atmosphere reservoir.

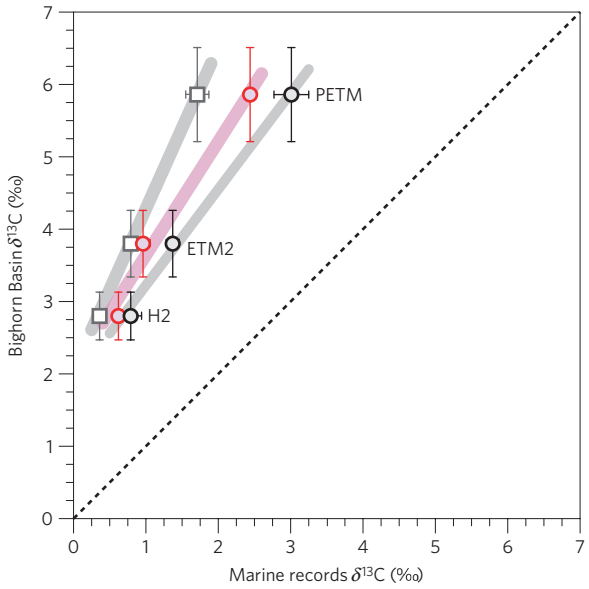

Figure 3 | Comparison of carbon isotope excursions for PETM, ETM2 and H2 for Bighorn Basin continental and different marine records. Marine data are from bulk carbonate from Mead and Dee Stream sections in New Zealand[17,27,28] (squares), ODP Site 1265 bulk carbonate (red circles) and Site 1263 (PETM) and Site 1267 (ETM2/H2) benthic foraminifer *N. truempyi* (black circles) from Walvis Ridge in the southern Atlantic Ocean[7,8,26]. Uncertainty intervals represent standard errors (1σ of the mean difference between baseline and excursion values; see Supplementary Table S6). The similar scaling between CIE amplitudes implies that the factors influencing CIE amplitudes for the different proxies reacted proportionally to the carbon input to the ocean–atmosphere carbon pool.

palaeoenvironmental change (causing the terrestrial amplification and/or oceanic dampening of the CIEs) and the amount of isotopically-light carbon added to the ocean–atmosphere system. The most parsimonious explanation for this proportionality is that atmospheric pCO_2 change scaled linearly with CIE magnitude across the three events. If true, this result implies that the isotopic composition of the carbon, and probably also the source(s) of carbon fuelling the events, were similar for the three hyperthermals[8,17]. The observed relationship between the terrestrial and marine CIEs does not intercept the origin, implying either a nonlinear relationship between carbon release and local environmental change or the existence of further environmental forcing factors that did not contribute to the CIEs. A large number of mechanisms are possible and should be evaluated in the future using Earth System models[11,13].

In contrast, if these hyperthermals were fuelled by different carbon sources, changes in pCO_2, and local palaeoenvironmental change, their CIE expressions in different marine and continental proxies would almost certainly scale inconsistently. Our finding of proportionality between pCO_2 increase and local palaeoenvironmental change during the PETM, ETM2 and H2 is in line with a similar covariance of benthic foraminiferal δ^{13}C (representing carbon cycle perturbation) and δ^{18}O (representing ocean water warming) values found for the three hyperthermals[8]. The much younger C22n-H3 and C21r-H1 events, which are recorded in the western Atlantic[4], show the same δ^{13}C/δ^{18}O covariance, suggesting that similar sources of carbon may have contributed to these events, as well.

The similar CIE scaling suggests that oceanic and/or terrestrial palaeoenvironmental changes that modulated CIE amplitude reacted similarly and proportionally to the magnitude of the three events. The impacts of the three events on mammalian faunas, however, do not seem to scale the same way. Whereas the PETM triggered dramatic holarctic dispersal of mammals causing fundamental reorganization of Bighorn Basin faunas[3,9], ETM2 and H2 occur stratigraphically above the next largest faunal event in the early Eocene Bighorn Basin record (Biohorizon B) and do not seem to be associated with noticeable mammalian turnover. This implies a nonlinear relationship between climatic and mammalian faunal change and suggests that biotic drivers or the crossing of climate thresholds, rather than climate change itself, are important in driving biotic turnover at Biohorizon B. Our result supports the view that macroevolutionary dynamics depend on the interaction between species' ecology and changing climate[30].

Received 1 September 2011; accepted 22 February 2012; published online 1 April 2012

References

1. Lourens, L. J. *et al.* Astronomical pacing of late Palaeocene to early Eocene global warming events. *Nature* **435,** 1083–1087 (2005).
2. Zachos, J. C., Dickens, G. R. & Zeebe, R. E. An early Cenozoic perspective on greenhouse warming and carbon-cycle dynamics. *Nature* **451,** 279–283 (2008).
3. Koch, P. L., Zachos, J. C. & Gingerich, P. D. Correlation between isotope records in marine and continental carbon reservoirs near the Palaeocene/Eocene boundary. *Nature* **358,** 319–322 (1992).
4. Sexton, P. F. *et al.* Eocene global warming events driven by ventilation of oceanic dissolved organic carbon. *Nature* **471,** 349–352 (2011).

5. Dickens, G. Down the rabbit hole: Toward appropriate discussion of methane release from gas hydrate systems during the Paleocene–Eocene Thermal Maximum and other past hyperthermal events. *Clim. Past* **7,** 831–846 (2011).
6. Cramer, B. S., Wright, J. D., Kent, D. V. & Aubry, M-P. Orbital climate forcing of $\delta^{13}C$ excursions in the late Paleocene–early Eocene (chrons C24n–C25n). *Paleoceanography* **18,** PA1097 (2003).
7. Stap, L., Sluijs, A., Thomas, E. & Lourens, L. J. Patterns and magnitude of deep sea carbonate dissolution during Eocene Thermal Maximum 2 and H2, Walvis Ridge, southeastern Atlantic Ocean. *Paleoceanography* **24,** PA1211 (2009).
8. Stap, L. *et al*. High-resolution deep-sea carbon and oxygen isotope records of Eocene Thermal Maximum 2 and H2. *Geology* **38,** 607–610 (2010).
9. Clyde, W. C. & Gingerich, P. D. Mammalian community response to the latest Paleocene thermal maximum: An isotaphonomic study in the northern Bighorn Basin, Wyoming. *Geology* **26,** 1011–1014 (1998).
10. Bowen, G. J. *et al*. Mammalian dispersal at the Paleocene/Eocene boundary. *Science* **295,** 2062–2065 (2002).
11. Zeebe, R. E., Zachos, J. C. & Dickens, G. R. Carbon dioxide forcing alone insufficient to explain Palaeocene–Eocene Thermal Maximum warming. *Nature Geosci.* **2,** 576–580 (2009).
12. McInerney, F. A. & Wing, S. L. The Paleocene–Eocene Thermal Maximum: A perturbation of carbon cycle, climate, and biosphere with implications for the future. *Annu. Rev. Earth Planet. Sci.* **39,** 489–516 (2011).
13. Panchuk, K., Ridgwell, A. & Kump, L. R. Sedimentary response to Paleocene–Eocene Thermal Maximum carbon release: A model-data comparison. *Geology* **36,** 315–318 (2008).
14. Bowen, G. J., Beerling, D. J., Koch, P. L., Zachos, J. C. & Quattlebaum, T. A humid climate state during the Paleocene–Eocene Thermal Maximum. *Nature* **432,** 495–499 (2004).
15. Wing, S. L. *et al*. Transient floral change and rapid global warming at the Paleocene–Eocene boundary. *Science* **310,** 993–996 (2005).
16. Sluijs, A. *et al*. Warm and wet conditions in the Arctic region during Eocene Thermal Maximum 2. *Nature Geosci.* **2,** 777–780 (2009).
17. Nicolo, M. J., Dickens, G. R., Hollis, C. J. & Zachos, J. C. Multiple early Eocene hyperthermals: Their sedimentary expression on the New Zealand continental margin and in the deep sea. *Geology* **35,** 699–702 (2007).
18. Abdul Aziz, H. *et al*. Astronomical climate control on paleosol stacking patterns in the upper Paleocene–lower Eocene Willwood Formation, Bighorn Basin, Wyoming. *Geology* **36,** 531–534 (2008).
19. Kraus, M. J. & Riggins, S. Transient drying during the Paleocene–Eocene Thermal Maximum (PETM): Analysis of paleosols in the Bighorn Basin, Wyoming. *Palaeogeogr. Palaeoclimatol. Palaeoecol.* **245,** 444–461 (2007).
20. Bowen, G. J. *et al*. in *Paleocene–Eocene Stratigraphy and Biotic Change in the Bighorn and Clark Fork Basins, Wyoming* (ed. Gingerich, P. D.) 73–88 (Papers on Paleontology 33, Univ. Michigan, 2001).
21. Clyde, W. C. *et al*. Basin-wide magnetostratigraphic framework for the Bighorn Basin, Wyoming. *GSA Bull.* **119,** 848–859 (2007).
22. Clementz, M. Early Eocene warming events and the timing of terrestrial faunal exchange between India and Asia. *Geology* **39,** 15–18 (2011).
23. Schankler, D. M. in *Early Cenozoic Paleontology and Stratigraphy of the Bighorn Basin, Wyoming* (ed. Gingerich, P. D.) 99–114 (Papers on Paleontology 24, Univ. Michigan, 1980).
24. Chew, A. Paleoecology of the early Eocene Willwood mammal fauna from the central Bighorn Basin, Wyoming. *Paleobiology* **35,** 13–31 (2009).
25. Westerhold, T. *et al*. On the duration of magnetochrons C24r and C25n and the timing of early Eocene global warming events: Implications from the Ocean Drilling Program Leg 208 Walvis Ridge depth transect. *Paleoceanography* **22,** PA2201 (2007).
26. McCarren, H., Thomas, E., Hasegawa, T., Röhl, U. & Zachos, J. C. Depth dependency of the Paleocene–Eocene carbon isotope excursion: Paired benthic and terrestrial biomarker records (Ocean Drilling Program Leg 208, Walvis Ridge). *Geochem. Geophys. Geosys.* **9,** Q10008 (2008).
27. Hollis, C. J., Dickens, G. R., Field, B. D., Jones, C. M. & Strong, C. P. The Paleocene–Eocene transition at Mead Stream, New Zealand: a southern Pacific record of early Cenozoic global change. *Palaeogeogr. Palaeocl. Palaeoecol.* **215,** 313–343 (2005).
28. Hancock, H. J. L., Dickens, G. R., Strong, C. P., Hollis, C. J. & Field, B. D. Foraminiferal and carbon isotope stratigraphy through the Paleocene–Eocene transition at Dee Stream, Marlborough, New Zealand. *New Zealand J. Geol. Geophys.* **46,** 1–19 (2003).
29. Uchikawa, J. & Zeebe, R. E. Examining possible effects of seawater pH decline on foraminiferal stable isotopes during the Paleocene–Eocene Thermal Maximum. *Paleoceanography* **25,** PA2216 (2010).
30. Ezard, T. H., Aze, T., Pearson, P. N. & Purvis, A. Interplay between changing climate and species' ecology drives macroevolutionary dynamics. *Science* **332,** 349–351 (2011).

Acknowledgements

This research was funded by a Netherlands Organisation for Scientific Research (NWO) Earth and Life Sciences (ALW) grant to H.A.A., National Science Foundation grants EAR-0707415 and EAR-0958821 to W.C.C., and EAR-0628302 and OCE-0902882 to G.J.B. We thank the Churchill family in Wyoming for logistical support, P. van den Berg, M. Clementz, J. Fahlke, D. and M. Gingerich, Sander, Sigrid and Sybren Hilgen, M. Hoerner, P. Lind, H. Miller, A. Sluijs and D. Wolf for helping with field work, and T. Barnum, A. Dangremond, A. van Dijk and W. Krijgsman for laboratory assistance.

Author contributions

H.A.A., W.C.C., P.D.G., F.J.H. and H.C.F. carried out fieldwork. H.A.A., W.C.C. and H.C.F. performed the laboratory analysis. H.A.A., W.C.C., P.D.G., H.C.F. and L.J.L. performed data integration. All authors contributed to the manuscript.

Additional information

The authors declare no competing financial interests. Supplementary information accompanies this paper on www.nature.com/naturegeoscience. Reprints and permissions information is available online at www.nature.com/reprints. Correspondence and requests for materials should be addressed to H.A.A.